Biol Cybern (2010) 102:57–69
DOI 10.1007/s00422-009-0350-5

ORIGINAL PAPER

Biological Cybernetics

Evaluating the effective connectivity of resting state networks using conditional Granger causality

Wei Liao · Dante Mantini · Zhiqiang Zhang · Zhengyong Pan · Jurong Ding · Qiyong Gong · Yihong Yang · Huafu Chen

Received: 1 June 2009 / Accepted: 10 November 2009 / Published online: 25 November 2009

Abstract The human brain has been documented to be spatially organized in a finite set of specific coherent patterns, namely resting state networks (RSNs). The interactions among RSNs, being potentially dynamic and directional, may not be adequately captured by simple correlation or anticorrelation. In order to evaluate the possible effective connectivity within those RSNs, we applied a conditional Granger causality analysis (CGCA) to the RSNs retrieved by independent component analysis (ICA) from resting state functional magnetic resonance imaging (fMRI) data. Our analysis provided evidence for specific causal influences among the detected RSNs: default-mode, dorsal attention, core, central-executive, self-referential, somatosensory, visual, and auditory networks. In particular, we identified that self-referential and default-mode networks (DMNs) play distinct and crucial roles in the human brain functional architecture. Specifically, the former RSN exerted the strongest causal influence over the other RSNs, revealing a top-down modulation of self-referential mental activity (SRN) over sensory and cognitive processing. In quite contrast, the latter RSN was profoundly affected by the other RSNs, which may underlie an integration of information from primary function and higher level cognition networks, consistent with previous task-related studies. Overall, our results revealed the causal influences among these RSNs at different processing levels, and supplied information for a deeper understanding of the brain network dynamics.

Keywords Resting state networks · Effective connectivity · Independent component analysis · Conditional Granger causality analysis

Electronic supplementary material The online version of this article (doi:10.1007/s00422-009-0350-5) contains supplementary material, which is available to authorized users.

Wei Liao and Dante Mantini contribute equally to this work.

W. Liao · Z. Pan · J. Ding · H. Chen (✉)
Key Laboratory for Neuroinformation of Ministry of Education, School of Life Science and Technology, University of Electronic Science and Technology of China, Chengdu 610054, People's Republic of China
e-mail: chenhf@uestc.edu.cn

D. Mantini
Institute for Advanced Biomedical Technologies, G. D'Annunzio University Foundation, Chieti, Italy

D. Mantini
Department of Clinical Sciences and Bio-imaging, G. D'Annunzio University, Chieti, Italy

D. Mantini
Laboratory for Neuro-Psychophysiology, K.U. Leuven Medical School, Leuven, Belgium

Z. Zhang
Department of Medical Imaging, Nanjing Jinling Hospital, Clinical School, Medical College, Nanjing University, Nanjing 210002, People's Republic of China

Q. Gong
Huaxi MR Research Center (HMRRC), Department of Radiology, West China Hospital of Sichuan University, West China School of Medicine, Chengdu 610041, People's Republic of China

Y. Yang
Neuroimaging Research Branch, National Institute on Drug Abuse, National Institutes of Health, Baltimore, MD, USA

1 Introduction

Exploring long-range interactions of neuronal assemblies at different temporal and spatial scales is an important issue in human brain research. The concept of brain functional

connectivity, defined as the statistical dependence between neuronal activities in distant regions, is central for the understanding of the organized behavior of cortical regions which constitute distributed functional networks typically engaged in cognitive and perceptive processing (Friston et al. 1996). Besides, activity in a neural system can directly or indirectly exert influence over that in another. This influence is modeled as effective connectivity in the brain (Friston 1994; Friston et al. 1993), and has been extensively investigated with multimodal functional neuroimaging studies (Brovelli et al. 2004; Seth 2005).

Functional magnetic resonance imaging (fMRI) has emerged as a powerful imaging tool for mapping the large-scale brain networks engaged in specific tasks or at rest. The original formulation of functional connectivity (in brain imaging) used principal component analysis (PCA) (Friston et al. 1993) to determine spatial patterns of coherent activity. In several recent studies, however, networks of interest are defined based on the correlation of the fMRI blood oxygen level-dependent (BOLD) signals of all the voxels of the brain with the mean time-course of a user-selected "seed" region (Biswal et al. 1995; Fox et al. 2005; Hampson et al. 2002). Interestingly, in analogy with PCA, independent component analysis (ICA), a data-driven method able to separate independent spatio-temporal patterns of coherent neuronal activity without prior knowledge about activity waveforms or locations (Bartels and Zeki 2005; McKeown et al. 1998; van de Ven et al. 2004), is becoming an increasing popular exploratory method for investigating functional connectivity, particularly in resting state fMRI data (Beckmann et al. 2005; Damoiseaux et al. 2006; De Luca et al. 2006; Mantini et al. 2007; Stevens et al. 2009; van de Ven et al. 2004).

Functional connectivity investigations documented that brain activity at rest is spatially organized in a finite set of specific coherent patterns (Damoiseaux et al. 2006; De Luca et al. 2006; Mantini et al. 2007). Interestingly, such patterns, namely resting state networks (RSNs), recapitulate the functional architecture of somato-motor, visual, auditory, attention, language, and memory networks that are commonly modulated during active behavioral tasks (Bartels and Zeki 2005; Corbetta and Shulman 2002; Gusnard and Raichle 2001). Despite there is not a consensus yet, a number of consistent RSNs, as detected by ICA, could be jointly reported in the same study, i.e., the default-mode network (DMN) (Gusnard et al. 2001; Gusnard and Raichle 2001; Raichle et al. 2001), and other task-positive networks corresponding to dorsal attention, visual, auditory, and sensorimotor processing (Beckmann et al. 2005; Chen et al. 2008; Damoiseaux et al. 2006; De Luca et al. 2006; Mantini et al. 2007; van de Ven et al. 2008). Interactions among these RSNs are still largely unexplored (Kelly et al. 2008). For example, the sensory systems, including the visual, auditory, and somatosensory networks, are anticorrelated with the DMN individually, but no positive correlation is found among them (Tian et al. 2007). Although competitive interactions have been documented even in the resting state between the DMN and the dorsal attention network (DAN) (Fox et al. 2005; Fransson 2005), it is debated whether this result is an effect of different brain systems competing for resources (Fox et al. 2009) or is purely induced by preprocessing for functional connectivity analysis (Murphy et al. 2009). In this study, we considered causality analysis to be particularly relevant to the investigation of the possible effective connectivity within RSNs, assuming that their interactions are complex, possibly dynamic and directional (Sridharan et al. 2008), rather than simple correlation, or anticorrelation. As a further remark, we would like to point out that the causality analysis should be substantially insensitive to the problem of possible false instantaneous interactions among RSNs. Specifically, its results should be unaffected by the factors that can theoretically induce temporal correlations between the RSN time-courses, such as the contamination of nonneural signals in the fMRI data, or the use of processing methods for their attenuation (Murphy et al. 2009).

In a causality study based on resting state fMRI, Jafri et al. (2008) addressed the temporally maximal correlation among these RSNs by using a delay correlation technique, and attempted to reveal the weaker temporal dependencies among these RSNs. However, the delay correlation method provides estimation of the dependencies between functional networks, but not the direct information of their causality. Alternatively, the Granger causality analysis (GCA) is likely to be an appropriate approach to study the directional interactions of these RSNs (Stevens et al. 2009). GCA rests upon multivariate or vector autoregressive models for fMRI time-series to test for directed connections (Harrison et al. 2003). The GCA can provide information about the dynamics and directionality of fMRI BOLD signal in cortical circuits (Chen et al. 2009; Gao et al. 2008; Goebel et al. 2003; Liao et al. 2009; Londei et al. 2007; Roebroeck et al. 2005; Seth 2005; Sridharan et al. 2008; Uddin et al. 2009; Upadhyay et al. 2008; Wilke et al. 2009; Zhou et al. 2009). The GCA, however, has the principal limit of dealing with bivariate time-series, which does not make use of the whole covariance structure for multivariate data. Another important extension of Granger's original definition of causality is the consideration of the multivariate case: For three or more simultaneous time series, the causal relation between any two of the series may be direct, mediated by a third one, or a combination of both. Recently, the conditional Granger causality analysis (CGCA) (Geweke 1984) has been proposed to estimate functional coupling effectively in multivariate data sets (Chen et al. 2006; Zhou et al. 2009).

Moreover, the functions in human brain are thought to be processed hierarchically, on the basis of either top-down or bottom-up modulation (Northoff et al. 2006). In this sense,

the RSNs representing the sensory system, including the visual, auditory, and somatosensory network, can be considered at the lower-order of the cognitive processing hierarchy; the RSNs corresponding to the DAN at higher-order processing; the DMN at the middle order (Northoff et al. 2006). From this standpoint, effective connectivity measures should be able to extract the strength and directionality of the network interactions, thus, allowing to assess the suitability of the aforementioned classification.

In this study, we have studied the possible effective connectivity within these RSNs, applying the CGCA to the temporal information of RSNs defined by ICA. In particular, we focused our interest on directed influences among the RSNs, because, as mentioned earlier, the instantaneous influence term of the CGCA may not provide clear evidence for RSN interactions at the neuronal level. Our approach is expected to reveal the causal influence among the RSNs at different cognitive processing hierarchy, supplying information for a deeper understanding of the brain network dynamics.

2 Materials and methods

2.1 Subjects

Twenty-two (nine women, age range: 21–42 years, mean age: 25.8 years) right-handed subjects participated in this study. All the subjects were healthy, with no history of psychiatric or neurologic illness. This study was approved by the local ethical committee in West China Hospital of Sichuan University, and informed written consent was obtained from all the subjects prior to the experiment. For the resting state scans, subjects were instructed simply to rest with their eyes closed, not to think of anything in particular, and not to fall asleep.

2.2 Data acquisition

Experiments were performed on a 3.0-T GE-Signa MRI scanner (EXCITE, General Electric, Milwaukee, USA) in Huaxi MR Research Center, Chengdu, China. Foam padding was used to minimize head motion for all the subjects. Functional images were acquired using a single-shot, gradient-recalled echo-planar imaging (EPI) sequence (TR = 1,000 ms, TE = 30 ms and flip angle = 90°). Sixteen transverse slices (FOV = 24 cm, in-plane matrix = 64 × 64, slice thickness = 6 mm, without gap), aligned along the anterior commissure–posterior commissure (AC–PC) line were acquired. Here, the scanner parameters were optimized for fast scanning, especially for shorter TR, which is very important for the analysis Granger causality on the time-courses (Roebroeck et al. 2005). For each subject, a total of 205 volumes was acquired, and the first five volumes were discarded to ensure steady-state longitudinal magnetization. Subsequently, for spatial normalization and localization, a set of high-resolution T1-weighted anatomic images was acquired in axial orientation using a 3D spoiled gradient recalled (SPGR) sequence (TR = 8.5 ms, TE = 3.4 ms, flip angle = 12°, matrix size = 512 × 512 × 156, and voxel size = $0.47 \times 0.47 \times 1\,\text{mm}^3$) on each subject.

2.3 Data preprocessing

Data preprocessing was partly carried out using the Statistical Parametric Mapping software (SPM2, http://www.fil.ion.ucl.ac.uk/spm). The 200 volumes were first corrected for the temporal difference in acquisition among different slices, and then the images were realigned to the first volume for head-motion correction. No subject's translational or rotational parameters in a data set exceeded ±1 mm or ±1°, and therefore, no datasets were excluded from the analysis. The fMRI images were realigned with the corresponding T1-volume and warped into a standard stereotaxic space at a resolution of $3 \times 3 \times 3\,\text{mm}^3$, using the Montreal Neurological Institute (MNI) EPI template in SPM2. Then, they were spatially smoothed by convolution with an isotropic Gaussian kernel (FWHM = 8 mm).

2.4 Independent component analysis

Group spatial ICA was conducted using the GIFT software (http://icatb.sourceforge.net/, version 1.3e) (Calhoun et al. 2001). This involves a preliminary dimension estimation on all the subjects to determine the number of independent components (ICs), using the minimum description length (MDL) criterion (Jafri et al. 2008; Li et al. 2007). Then, fMRI data from all the subjects were concatenated, and the temporal dimension of this aggregate data set was reduced to 40 by means of PCA (see Supplementary Fig. 1), followed by an IC (with time-courses and spatial maps) estimation using the FastICA algorithm (Hyvarinen 1999). IC time-courses and spatial maps for each subject were back-reconstructed, using the aggregated components and the results from the data reduction step (Calhoun et al. 2001; Jafri et al. 2008). For each IC, the time-course corresponds to the waveform of a specific pattern of coherent brain activity, and the intensity of this pattern of brain activity across the voxels is expressed in the associated spatial map (Mantini et al. 2007). In order to display the voxels that contributed most strongly to a particular IC, the intensity values in each spatial map were converted to Z-values, removing the average value and dividing by the standard deviation of the intensity distribution (Calhoun et al. 2001; Mantini et al. 2007). Voxels with absolute Z-values greater than a preset threshold (in this study, $|Z| > 1.5$) are considered active voxels of the IC. Negative Z-values

indicate voxels in which the BOLD signals are modulated opposite to the IC time-course (Mantini et al. 2007).

2.5 RSN detection

According to the previous studies (Jafri et al. 2008; Stevens et al. 2007), a selection of the components to be retained for further analysis among the 40 estimated ICs was performed using anatomic information. The classification of the ICs in terms of RSNs was performed according to the fMRI networks during rest consistently shown in previous ICA studies (Beckmann et al. 2005; Damoiseaux et al. 2006; De Luca et al. 2006; Mantini et al. 2007), using the network spatial maps from our previous studies (Mantini et al. 2007, 2009). Specifically, our selected RSNs corresponded to the cerebral ICs with the largest spatial correlations with the network templates (van de Ven et al. 2004, 2008).

2.6 Frequency analysis of RSN time-courses

Spatial ICA in GIFT produced time-courses for each IC and for each subject. Prior to investigating the effective connectivity relationship among the selected RSNs, their time-courses were analyzed in the frequency domain, and subsequently filtered through a band-pass filter at low-frequency bands (0.005–0.17 Hz), according to the method by Salvador et al. (2005), to reduce the effects of low-frequency drift and high-frequency noise.

2.7 Conditional Granger causality analysis

CGCA is based on a straightforward expansion of the autoregressive model to a general multivariate case including all measured variables. CGCA was introduced by Geweke (1984), as recently reviewed in Chen et al. (2006) and applied to fMRI data (Zhou et al. 2009). Consider the case of three time-courses X_t, Y_t, and Z_t. First, the joint autoregressive representation for X_t and Z_t can be written as

$$\begin{aligned} X_t &= \sum_{j=1}^{p} a_{1j} X_{t-j} + \sum_{j=1}^{p} b_{1j} Z_{t-j} + \varepsilon_{1t}, \\ Z_t &= \sum_{j=1}^{p} c_{1j} X_{t-j} + \sum_{j=1}^{p} d_{1j} Z_{t-j} + \varepsilon_{2t}, \end{aligned} \tag{1}$$

and the noise covariance matrix can be represented as

$$\sum\nolimits_1 = \begin{pmatrix} \mathrm{var}(\varepsilon_{1t}) & \mathrm{cov}(\varepsilon_{1t}, \varepsilon_{2t}) \\ \mathrm{cov}(\varepsilon_{2t}, \varepsilon_{1t}) & \mathrm{var}(\varepsilon_{2t}) \end{pmatrix}. \tag{2}$$

Next, we consider the joint autoregressive representation for a system involving all the three time-courses X_t, Y_t, and Z_t as

$$\begin{aligned} X_t &= \sum_{j=1}^{p} a_{2j} X_{t-j} + \sum_{j=1}^{p} b_{2j} Y_{t-j} + \sum_{j=1}^{p} c_{2j} Z_{t-j} + \varepsilon_{3t}, \\ Y_t &= \sum_{j=1}^{p} d_{2j} X_{t-j} + \sum_{j=1}^{p} e_{2j} Y_{t-j} + \sum_{j=1}^{p} f_{2j} Z_{t-j} + \varepsilon_{4j}, \\ Z_t &= \sum_{j=1}^{p} g_{2j} X_{t-j} + \sum_{j=1}^{p} h_{2j} Y_{t-j} + \sum_{j=1}^{p} k_{2j} Z_{t-j} + \varepsilon_{5j}, \end{aligned} \tag{3}$$

and the noise covariance matrix for the above system can be represented as

$$\sum\nolimits_2 = \begin{pmatrix} \mathrm{var}(\varepsilon_{3t}) & \mathrm{cov}(\varepsilon_{3t}, \varepsilon_{4t}) & \mathrm{cov}(\varepsilon_{3t}, \varepsilon_{5t}) \\ \mathrm{cov}(\varepsilon_{4t}, \varepsilon_{3t}) & \mathrm{var}(\varepsilon_{4t}) & \mathrm{cov}(\varepsilon_{4t}, \varepsilon_{5t}) \\ \mathrm{cov}(\varepsilon_{5t}, \varepsilon_{3t}) & \mathrm{cov}(\varepsilon_{5t}, \varepsilon_{5t}) & \mathrm{var}(\varepsilon_{5t}) \end{pmatrix} \tag{4}$$

where p is the order of the autoregressive model; and ε_{it}, $i = 1, \ldots, 5$ are the prediction error, which are uncorrelated over time. From these two sets of equations, we define the conditional Granger causality from time-course Y_t to X_t conditional on time-course Z_t as

$$F_{Y \to X|Z} = \ln \left(\frac{\mathrm{var}(\varepsilon_{1t})}{\mathrm{var}(\varepsilon_{3t})} \right). \tag{5}$$

It is worth pointing out that Eq. 5 is essentially a log likelihood ratio test, comparing models with and without the directed connection from Y_t to X_t. When the causal influence from time-course Y_t to X_t is entirely mediated by other time-course Z_t, the coefficients b_{2j} in Eq. 3 are uniformly zero, and $\mathrm{var}(\varepsilon_{1t}) = \mathrm{var}(\varepsilon_{3t})$. As such, $F_{Y \to X|Z} = 0$, meaning that no further improvement in the predication of time-course X_t can be expected by including past measurements of time-course Y_t conditioned on the other time-course Z_t. On the contrary, when a direct influence from time-course Y_t to X_t exists, the inclusion of past measurements of time-course Y_t in addition to that of time-course X_t and Z_t should result in better predictions of time-course X_t, leading to $\mathrm{var}(\varepsilon_{1t}) > \mathrm{var}(\varepsilon_{3t})$, and $F_{Y \to X|Z} > 0$ (Chen et al. 2006).

Applying the theory of CGCA to the resting state fMRI data, the time-course of one of the RSNs can be associated with X_t, and another one with Y_t. Z_t represents all the remaining RSN time-courses other than X_t and Y_t. Accordingly, CGCA was performed to test causal influences among RSNs using (1) the influence terms ($F_{X \to Y|Z}$ and $F_{Y \to X|Z}$) (Gao et al. 2008; Goebel et al. 2003) and (2) the difference of influence term ($F_{X \to Y|Z} - F_{Y \to X|Z}$) (Roebroeck et al. 2005; Sridharan et al. 2008). The order of the autoregressive model was set to 1 using the Schwarz criterion (SC), although other order selection criteria could also be used (Akaike information criterion and Hannan–Quinn criterion). The coefficients of the models were calculated using a standard least squares optimization.

2.8 Node interaction analysis

In order to better extract information on the temporal relations among these RSNs obtained from CGCA, a node interaction analysis was performed. Significant Granger causality interactions on the difference of influence term ($F_{X\to Y|Z} - F_{Y\to X|Z}$) among these RSNs can be represented as edges in a graph, allowing the application of graph-theoretic techniques. We chose to base our graph theory analyses on the difference of influences, as opposed to the influences per se, because these were conserved more consistently over subjects. Since Granger causality is in general not symmetric, these edges are directional. A general definition of the CGCA graph-theoretic properties, as provided in previous studies (Seth 2005; Sridharan et al. 2008; Stevens et al. 2009), is listed in the following:

- *Out-degree*: Number of Granger causal afferent connections from a node (one of the RSNs) to any other node.
- *In-degree*: Number of Granger causal efferent connections to a node from any other node.
- (*Out-In*) *degree*: Difference between the out-degree and in-degree as a measure of the causal flow associated with a node. This casual flow profile identifies nodes that differentially affect, or are affected by, the other ones. A node with highly positive casual flow (Out-In degree) exerts a strong causal influence. On the contrary, a node with negative casual flow (Out-In degree) can be considered to be largely affected by the other ones.
- *Path length*: Shortest path from a node to every other node in the Granger causality network (normalized by the number of nodes minus one). A shorter path length indicates a more strongly interconnected or hub node (Stam and Reijneveld 2007). The path length was computed using the Dijkstra's shortest path algorithm (Sridharan et al. 2008).

In this study, we constructed and analyzed the distribution of these graph-theoretic properties, for each node of the Granger causality network, also calculating the mean value and standard error across all the subjects (Sridharan et al. 2008). As not all the graph-theoretic properties of the RSNs showed Gaussian distribution, the Mann–Whitney U test applied here to identify those nodes with graph-theoretic properties is significantly different ($P < 0.05$, FDR corrected for multiple comparisons) from the others in the Granger causality network.

3 Results

3.1 Component selection and analysis

The number of ICs in the resting state fMRI data was estimated to be approximately 40 from the MDL analysis (Supplementary Fig. 1). Accordingly, this output dimensionality was used for the ICA decomposition.

The spatial maps of the eight RSNs obtained with this analysis are illustrated in Fig. 1. Supplementary Table 1 summarizes for each RSN the active regions and the MNI coordinates of the peak foci, as well as the associated Brodmann areas (BA). On the basis of our classification results, and those of a large number of RSN studies (Beckmann et al. 2005; Damoiseaux et al. 2006; De Luca et al. 2006; Jafri et al. 2008; Mantini et al. 2007; Stevens et al. 2009; van den Heuvel et al. 2008), the eight ICs associated to RSNs can be described as follows.

- *RSN 1*: a network of regions typically referred to as the DMN (Fox et al. 2005; Greicius et al. 2003; Gusnard et al. 2001; Gusnard and Raichle 2001; Raichle et al. 2001). This network has been suggested to be involved in episodic memory (Vincent et al. 2006), and self-projection (Buckner and Carroll 2007). It involves posterior cingulate cortex (PCC)/precuneus region, bilateral inferior parietal gyrus, angular gyrus, middle temporal gyrus, superior frontal gyrus and medial frontal gyrus.
- *RSN 2*: a network overlapping with the DAN, which is thought to mediate goal-directed top-down processing (Corbetta and Shulman 2002). The network, which is left-lateralized, primarily involves middle, and superior occipital gyrus, parietal gyrus, inferior and superior parietal gyrus, and middle and superior frontal gyrus.
- *RSN 3*: a right-lateralized network putatively associated with central-executive network (CEN) (Koechlin and Summerfield 2007; Sridharan et al. 2008), whose key regions include the dorsal lateral prefrontal cortices and the posterior parietal cortices.
- *RSN 4*: a network dedicated to visual processing (VN) (Lowe et al. 1998), which includes the inferior, middle and superior occipital gyrus, the temporal-occipital regions along with superior parietal gyrus.
- *RSN 5*: a network that primary encompasses the bilateral middle and superior temporal gyrus, Heschl gyrus, insular cortex, temporal pole, and correspond to the auditory system (AN) (Biswal et al. 1997; Eckert et al. 2008).
- *RSN 6*: a network corresponding to sensory-motor function (SMN) (Biswal et al. 1995; Fox et al. 2006). This network includes pre- and postcentral gyrus, the primary sensory-motor cortices, and the supplementary motor area.
- *RSN 7*: a network putatively related to SRN (D'Argembeau et al. 2005). It includes the ventromedial prefrontal cortex (vMPFC), medial orbital prefrontal cortex (MOPFC), gyrus rectus, and pregenual anterior cingulate gyrus (PACC).
- *RSN 8*: a network associated with task control function, namely core network (CN) (Dosenbach et al. 2006, 2007; Mantini et al. 2009) whose key regions include the anterior cingulate, the bilateral insular, and dorso-lateral prefrontal cortices.

The power spectra calculated from the RSN time-courses show that the frequency content is largely concentrated

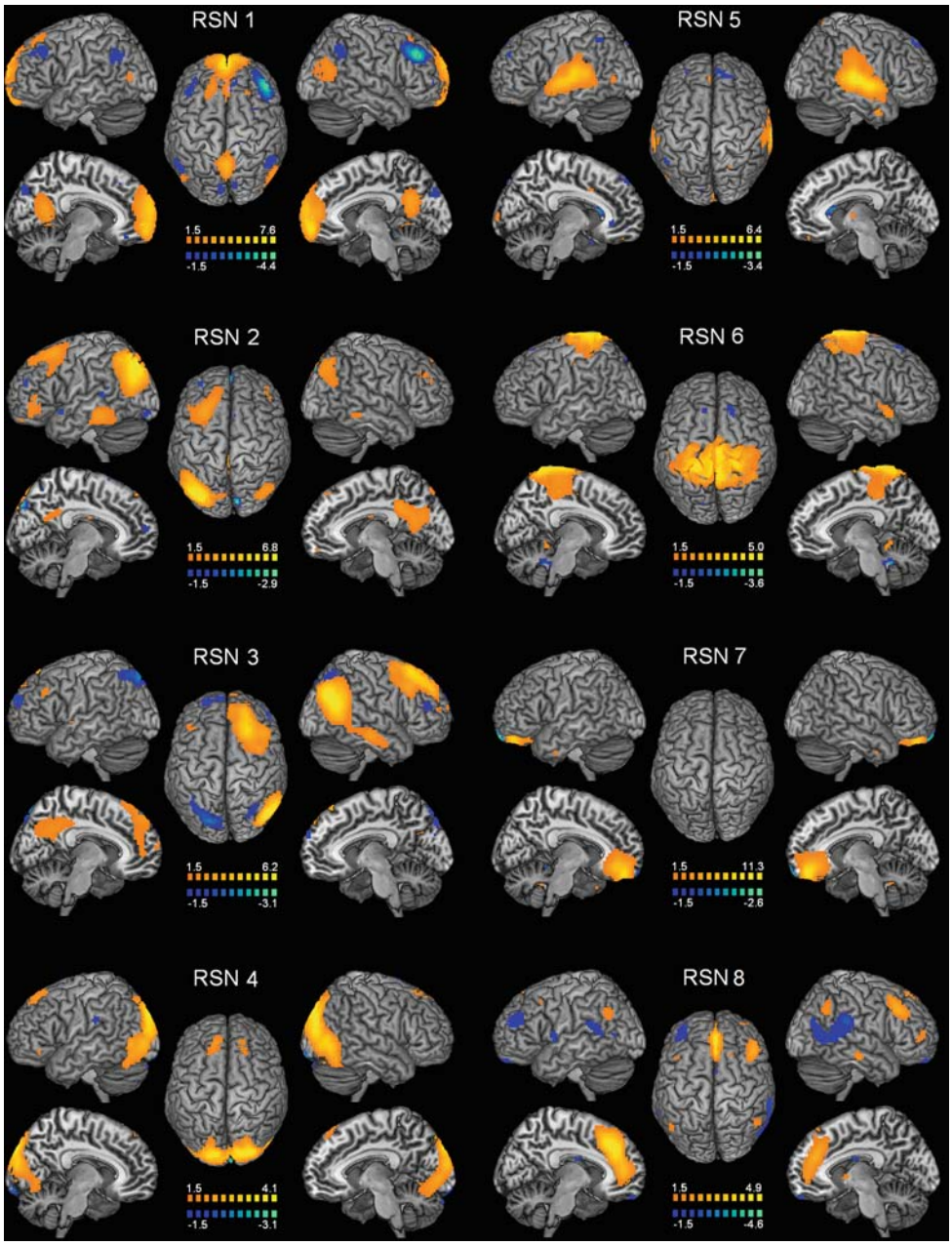

Fig. 1 Cortical representation of the eight RSNs of resting state fMRI data of a group results of 22 subjects. For each RSN. *Left*: Lateral and medial views of left hemisphere. *Center*: Dorsal view. *Right*: Lateral and medial views of right hemisphere

below 0.1 Hz (Fig. 2). It is observed that each RSN is characterized by a specific spectral profile, with one or more peaks. The DMN, the CEN, the SRN, and the DAN show a common peak in the frequency domain at 0.02 Hz. Moreover, the SMN shows a peak at 0.015 Hz. The RSNs with peaks at relatively higher frequency are the VN, AN, and CN. The VN shows three large peaks at 0.025, 0.045, and 0.7 Hz; the AN, a prominent peak at 0.04 Hz; the CN, two large peaks at 0.045 and 0.1 Hz.

3.2 Granger causality analysis

A Granger casual connectivity network was constructed (Fig. 2) in which the thickness of connecting arrows indicated the strengths of the causal influences in low frequency. Figure 3 shows the Granger casual connectivity measures of the eight RSNs, the slice activation maps of each RSNs, and the corresponding time-courses filtered with low frequency band (0.005–0.17 Hz). The "raw" influence terms ($F_{X\to Y|Z}$ and $F_{Y\to X|Z}$) were normalized by the respective maximum F-value. We reported the raw F-values of the directed influence terms ($F_{X\to Y|Z}$ and $F_{Y\to X|Z}$) in Supplementary Table 2. Only links with significant directed influence terms ($F_{X\to Y|Z}$ and $F_{Y\to X|Z}$) at the group-level ($P < 0.05$, FDR corrected) are shown in gray arrows. Further, a subset of these casual connectivity arrows showing the difference of influence term ($F_{X\to Y|Z} - F_{Y\to X|Z}$) (dominant direction of influence) ($P < 0.05$, FDR corrected) is

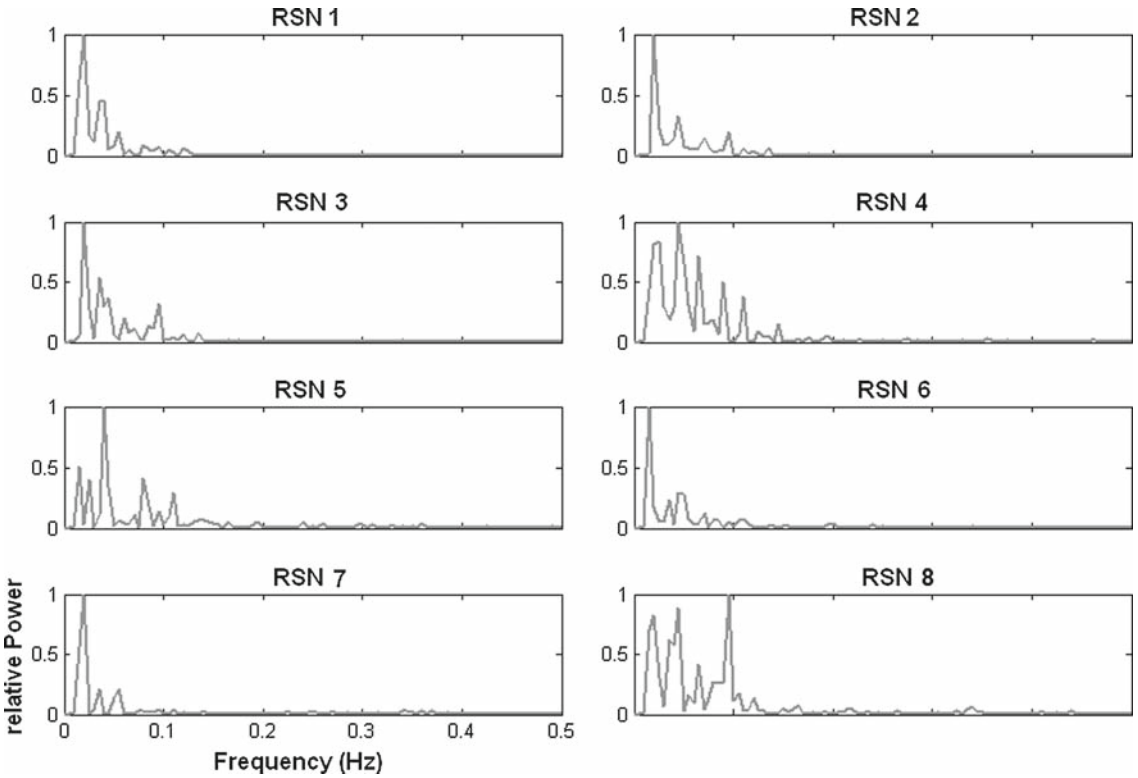

Fig. 2 The frequency content of the RSN time-courses: RSN 1 with a peak in the frequency domain at 0.02 Hz; RSN 2 with a peak at 0.02 Hz; RSN 3 with a peak at 0.02 Hz; RSN 4 with a peak at 0.045 Hz; RSN 5 with a peak at 0.04 Hz; RSN 6 with a peak at 0.015 Hz; RSN 7 with a peak at 0.02 Hz; RSN 8 with a peak at 0.095 Hz

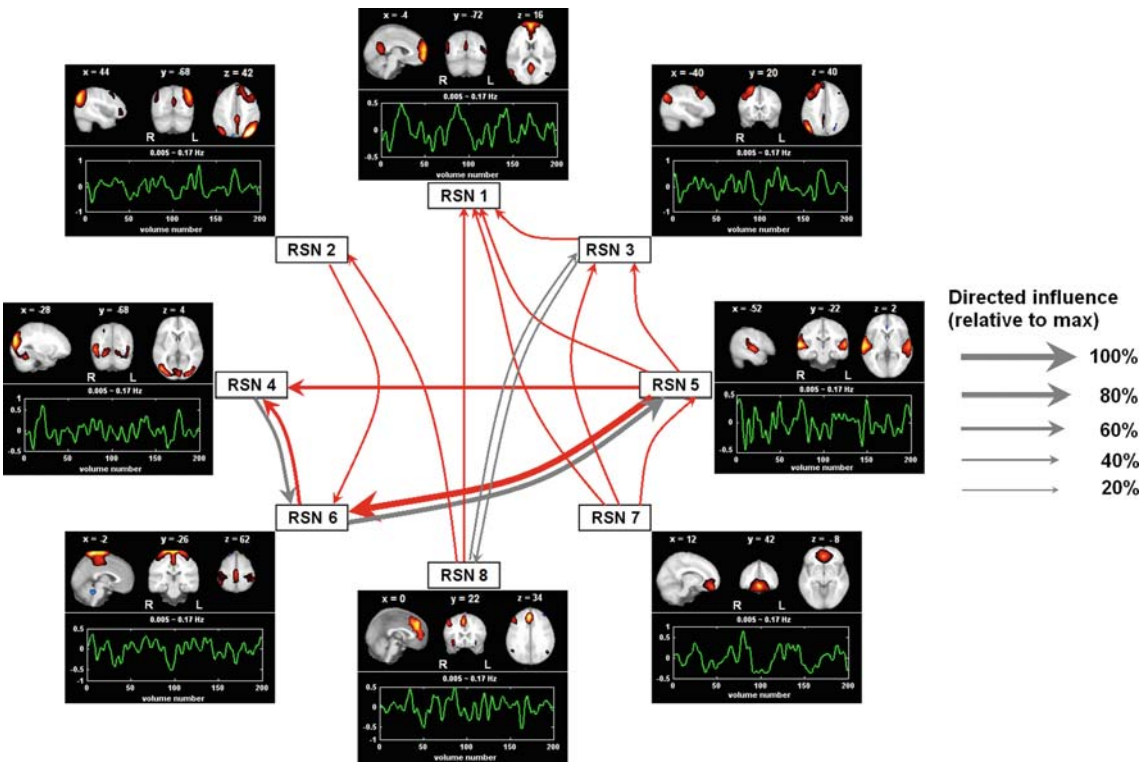

Fig. 3 Granger causality network of the eight RSNs during resting state on low frequency band (0.005–0.17 Hz), obtained from the CGCA

highlighted in red in the same figure (For interpretation of the references to colour in this figure legend, the reader is referred to the web version of this article.). The details of raw F-values of the difference of influence term ($F_{X\to Y|Z} - F_{Y\to X|Z}$) are provided in Supplementary Table 3.

In summary, a large number of Granger causal interactions were detected among RSNs. Interactions were predominantly directional, with bidirectional interactions only between AN and SMN, SMN and VN, and CEN and CN. Interestingly, DMN and SRN showed ingoing and outgoing interactions, respectively.

3.3 Node interaction analysis

In order to quantify the Granger casual interactions of each RSNs, key graph-theoretic properties were performed, and the distribution of these properties across subjects was constructed. Node interaction analysis on the difference of influence term ($F_{X\to y|Z} - F_{Y\to X|Z}$) identified with CGCA allowed quantifying the strength of causal afferent connections (Out-degree) (Supplementary Fig. 2), the strength of causal efferent connections (In-degree) (Supplementary Fig. 3), the difference between out-degree and in-degree (Out-In degree) (Fig. 4), and the shortest path length among all RSNs (means and standard errors of these properties are listed in Supplementary Table 4). The SRN (RSN 7) had the highest net causal flow (Out-In degree) among all the RSNs. Significant differences in net causal flow (Out-In degree) was showed between SRN and the DMN (RSN 1), DAN (RSN 2), CEN (RSN 3), and VN (RSN 4) (Mann–Whitney U test, $P < 0.05$, FDR corrected).

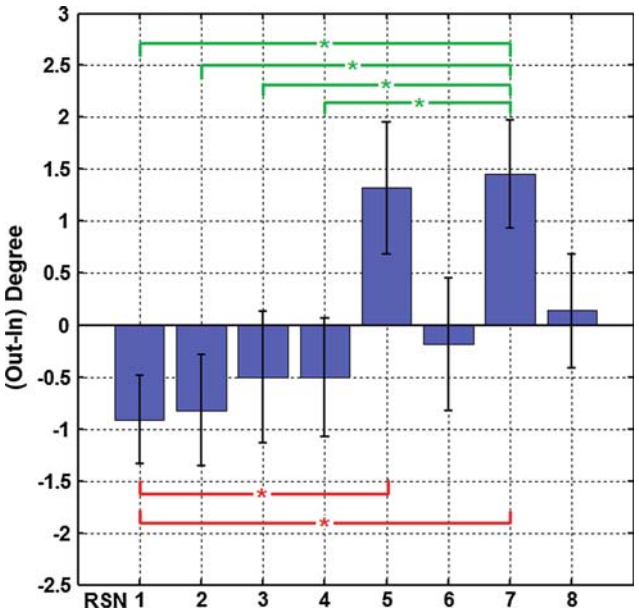

Fig. 4 Net Granger causal flow (Out-In degree) of all eight RSNs. Significant differences (marked with *asterisk*) in net causal flow between RSN 7 (SRN) and other RSNs statistically assessed with the Mann–Whitney U test ($P < 0.05$, FDR-corrected for multiple comparison), are indicated with upper lines. Similarly, significant differences in net Granger causal flow between RSN 1 (DMN) and other RSNs are shown with lower lines

4 Discussion

To the best of our knowledge, this is the first study in which effective connectivity among RSNs was examined using CGCA directly. We observed that: (1) specific and consistent causal influences among the RSNs are present in the human brain; (2) the detected causal influences between lower-order, middle order, and higher-order processing networks are in accordance with the concept of top-down or bottom-up modulation; and (3) the SRN and the DMN largely show efferent and afferent interactions with other RSNs, respectively. These results will be discussed in detail as follows.

4.1 Methodologic considerations

The use of functional connectivity analyses of fMRI data, which permits the study of coherent brain activity in distant brain areas, has gained acceptance in neuroscientific research. This approach is particularly valuable for the investigation of cerebral networks, for which results supporting a functional organization, not only related to task-induced processes (Bartels and Zeki 2005; McKiernan et al. 2003) but also to coherent synchronization/desynchronization processes ongoing even during rest (De Luca et al. 2006; Fox et al. 2005; Mantini et al. 2007), were reported.

A large number of functional imaging studies describing specific patterns of seed-based coherences across the human brain are present in the literature (Biswal et al. 1995, 1997; Cordes et al. 2000; Fox et al. 2005; Greicius et al. 2003; Hampson et al. 2002; Lowe et al. 1998). The analysis method used in these studies supplied a solid foundation for hypothesis-driven studies, which allowed the exploration of different functional patterns. However, in this study, we defined large-scale brain networks by means of ICA, a data-driven approach. ICA is a method capable of separating independent spatio-temporal patterns of synchronized neural activity from fMRI data (Bartels and Zeki 2005), without prior knowledge about their activity waveforms or locations (McKeown et al. 1998). Numerous authors demonstrated that voxels belonging to a given ICA network have higher BOLD temporal correlations among themselves compared with voxels belonging to other patterns, making ICA particularly suitable for functional connectivity studies (Beckmann et al. 2005; Chen et al. 2008; Damoiseaux et al. 2006; De Luca et al. 2006; Greicius et al. 2004; Jafri et al. 2008; Mantini et al. 2007; Stevens et al. 2009). Using ICA, we obtained reproducible

RSN spatial maps across subjects, along with their associated time-courses, which could be used for effective connectivity analysis.

A widely used approach for exploring effective connectivity properties in fMRI data is GCA, proposed and formalized by Granger (1969). GCA has already shown its effectiveness in evaluating direct, indirect, and instantaneous causal relationships among brain regions (Chen et al. 2009; Gao et al. 2008; Goebel et al. 2003; Liao et al. 2009; Londei et al. 2007; Roebroeck et al. 2005; Sridharan et al. 2008; Stevens et al. 2009; Uddin et al. 2009; Upadhyay et al. 2008; Wilke et al. 2009). However, there are some controversies whether it is appropriate to apply GCA to fMRI data (Friston 2009a,b; Roebroeck et al. 2009). In fact, there are some reasons why GCA might not be the method of choice for fMRI data. For example, the causal interactions are mediated at the neuronal level, and the vector autoregression models used by GCA have no hidden neuronal states. Another concern is the fact that GCA rests upon uncorrelated prediction errors, although random fluctuations in fMRI data are smooth because of the hemodynamic response convolution. Finally, regional variations in the latency of the hemodynamic response function would violate the assumptions of temporal precedence upon which GCA is based. In our current application, we can appeal to the fact that we are looking at the coupling among distributed modes, where any variations in hemodynamic latency will average out. Having said this, we have to qualify our interpretation that the influence among the RSNs that we have identified is due to neuronal activity only. The GCA approach is based upon a vector regression model with just two variables at one time: a seed region and another voxel. This means that such an assessment of effective connectivity ignored the influences of other areas, when assessing the coupling between the reference region and any particular voxel. However, if both brain regions A and B are driven by region C, but with a different lag, then there will be Granger causality between A and B (Gao et al. 2008). In order to handle this issue, an important extension of Granger's original definition of causality to the multivariate case, called CGCA, was proposed by Geweke (1984). For three or more simultaneous time-courses, the causal relation between any two of the courses may be direct, mediated by a third one, or a combination of both. Accordingly, CGCA is based on a straightforward expansion of the autoregressive model to a general multivariate case, including all measured variables. In our study, we applied CGCA to the RSN time-courses, to investigate the effective connectivity among cerebral networks in a resting state condition. Within this framework, more CGCA measures could be used, particularly the raw influence terms ($F_{X\to Y|Z}$ and $F_{Y\to X|Z}$) (Gao et al. 2008; Goebel et al. 2003) and the difference of influence term ($F_{X\to Y|Z} - F_{Y\to X|Z}$) (Roebroeck et al. 2005; Sridharan et al. 2008). Our results suggested a larger consistency in the estimation of the node interactions could be observed with the difference of influence term ($F_{X\to Y|Z} - F_{Y\to X|Z}$), which is likely to limit potentially spurious links caused by hemodynamic blurring (Roebroeck et al. 2005; Sridharan et al. 2008).

4.2 Analysis of resting state networks

We separated and characterized the activity of eight RSNs, which strongly overlapped with DMN, CEN, SRN, DAN, CN, VN, AN, and SMN, as previously defined in neuroimaging studies on active behavioral tasks (Corbetta and Shulman 2002; D'Argembeau et al. 2005; Dosenbach et al. 2006; Gusnard and Raichle 2001; Kwong et al. 1992; Seifritz et al. 2002). Our networks have been also reported in a number of previous resting state studies (Beckmann et al. 2005; Chen et al. 2008; Damoiseaux et al. 2006; De Luca et al. 2006; Mantini et al. 2007; van den Heuvel et al. 2008), although there is no complete consensus on the number and topology of the RSNs.

Our data provided evidence for the presence of two fronto-parietal lateralized networks that were putatively associated with the DAN, thought to mediate goal-directed stimulus-response selection (Corbetta and Shulman 2002), and with the CEN, assumed to be dedicated to adaptive task control (Dosenbach et al. 2007). This partition, previously reported by other authors (Beckmann et al. 2005; Chen et al. 2008; Damoiseaux et al. 2006), has been suggested to be largely related to hemispheric functional specialization (Damoiseaux et al. 2006). This issue has been addressed by Stark and coworkers, who studied the regional variation in interhemispheric coordination of spontaneous fMRI fluctuations (Stark et al. 2008). They observed a high degree of interhemispheric synchrony in primary sensory cortices, which is essential for bilateral sensory integration and motor coordination, and a lower degree of interhemispheric coordination in prefrontal and temporoparietal heteromodal association regions, reflecting the predisposition of higher-order homotopic regions to operate more independently.

Moreover, our results confirmed the separation provided by ICA between DMN and SRN, as previously reported in a simultaneous EEG-fMRI study by Mantini et al. (2007). As they observed hemodynamic fluctuations in these two RSNs to be related to power variations in alpha/beta and gamma rhythms, respectively, they suggested different neuronal mechanisms underlying their function. Interestingly, our causal connectivity results support this assumption, as will be discussed in detail in the following paragraphs.

Another important finding of this study is the characterization of the frequency content of the RSN fluctuations. Although it has been largely reported that intrinsic hemodynamic activity is predominantly present between 0.01 and 0.1 Hz (Cordes et al. 2001; Fox et al. 2005), as well as

frequency specificity across networks has been previously documented (Wu et al. 2008), we have even been able to provide a complete description of the RSN power spectra. Differently from the results of Mantini et al. (2007), which showed peaks at higher frequency for the dorsal attention with than for the DMN, we observed the DMN, the SRN, the DAN, and the CEN to show a common peak at 0.02 Hz. Furthermore, the CN, AN, and VN were found to have peaks at relatively higher frequency than the other RSNs. Possible discrepancies between these networks suggest that distinct physiologic mechanisms, perhaps related to differences in underlying neuronal activity, may coexist in these brain regions to sustain the network functions at rest.

4.3 Causal connectivity of self-referential network

Brain activity at rest is known to involve functional processes of different kinds, including monitoring of external environment and body state, stimulus-independent thought, planning and problem exclusive, and planning future actions (Gusnard and Raichle 2001). Among all these processes, SRN may play an important role (D'Argembeau et al. 2005; Northoff et al. 2006). SRN processing has been assumed to filter, select, and provide those stimuli which are relevant for the self of a particular person, so that self-referential processing can be regarded rather as intermediary between sensory and higher-order processing than a higher-order process by itself. The SRN (RSN 7) has already shown peculiar physiologic characteristics in the resting state, showing a high level of neural activity during resting conditions (Gusnard et al. 2001; Gusnard and Raichle 2001; Raichle et al. 2001). Particularly, D'Argembeau et al. (2005) have argued that the resting state is, indeed, characterized by a substantial amount of SRN, and have suggested that the resting state may enable people to represent knowledge concerning to themselves. Furthermore, previous task-related studies reported the SRN to be related self-knowledge (Macrae et al. 2004), self-material (Northoff and Bermpohl 2004) and SRN processing (D'Argembeau et al. 2005; for a recent meta-analysis see Northoff et al. 2006). Moreover, it has been provided evidence for areas within this network to allow for top-down modulation between sensory, self-referential, and higher-order processing (Northoff et al. 2006). For all the aforementioned reasons, the self-referential mental network can be reasonably assumed to be a hub, allowing for top-down modulation among all RSNs. Such a speculation is supported by our results, as this network had the highest net causal flow (Out-In degree) and the shortest path length among all the RSNs. This suggests, in a positive causal flow sense, that the SRN exerts a strong causal influence over the other RSNs.

More specifically, a dominant direction of the causal influence was detected from the SRN (RSN 7) to the DMN (RSN 1), the CEN (RSN 3), and the AN (RSN 5). The SRN includes ventromedial prefrontal cortex (vMPFC), MOPFC, PACC which, for convenience, will be jointly named as medial frontal cortex (MFC). Anatomically, most MFC projections are intrinsic or involved in neighboring prefrontal areas (Amodio and Frith 2006) (e.g., part of RSN 1 and RSN 3). MFC is also densely connected with the amygdala, the basal ganglia including the striatum and the nucleus accumbens, all primary exteroceptive sensory modalities, as well as subcortical regions implicated in interoceptive processing (Ongur and Price 2000). Further, there are major anatomic connects between MOPFC and the dorsolateral prefrontal cortex, temporal pole, anterior superior temporal gyrus, parietotemporal cortex, and PCC (these regions mostly emerge in RSNs 1, 2, 3, 5) (for detailed review, see Amodio and Frith 2006). In an fMRI resting state study, Uddin and colleagues found by means of a correlation-based approach that vMPFC may directly modulate activity in task-positive networks. In addition, they demonstrated by means of GCA that vMPFC negatively predicted activity in the CEN. This was interpreted as an evidence that vMPFC may directly bias the brain toward a less vigilant state at rest, requiring suppression to release task-control processes during task performance (Uddin et al. 2009).

4.4 Causal connectivity of default-mode network

The DMN exhibits high levels of activity during resting state and decreases the activity for processes of internal-oriented mental activity, such as mind wandering, episodic memory, and environmental monitoring (for a recent review see Buckner et al. 2008; Gusnard et al. 2001; Gusnard and Raichle 2001; Raichle et al. 2001). The DMN has been proposed to be a brain intrinsic system similar to the sensory-motor system or the visual system (Buckner et al. 2008). It involves several brain regions, such as PCC/precuneus region, bilateral inferior parietal gyrus, inferior temporal gyrus, and medial frontal gyrus (Gusnard et al. 2001; Gusnard and Raichle 2001; Raichle et al. 2001). These brain areas are tightly functionally connected and distinct from other brain areas. Graph-theory analysis by Achard et al. (2006) suggested that precuneus region, bilateral inferior parietal gyrus, inferior temporal gyrus, and medial frontal gyrus (most of areas in the DMN) are critical for cognition.

The DMN function is fundamental in the resting state, as this network can integrate information from RSNs related to both primary function and higher level cognition. In accordance with this hypothesis, our study showed the DMN to have the lowest negative net causal flow (Out-In degree), and more specifically to be affected by the SRN (RSN 7), the CEN (RSN 3), the AN (RSN 5), and the CN (RSN 8) (Fig. 3). Based on previous interpretation, one possibility is that DMN activity is associated with various forms of thought

involving multiple sensory and cognitive representations (Buckner et al. 2008). Another possibility is that spontaneous neuronal oscillations measured during resting state may reflect both intrinsic low-level physiologic processes and spontaneous cognitive events. The causal influences of the DMN by SRN (RSN 7) have been discussed in the previous section. Sridharan et al. (2008) using Granger causality documented that the CN (RSN 8) had an important role in cognitive control related to switching between the DMN and task-related networks as shown in our results, brain areas in the CN (RSN 8) affected the DMN during the resting state. A possible reason for the causal influences on the DMN by the CEN (RSN 3) is that the DMN plays an important role in monitoring the external environment (Buckner et al. 2008; Gusnard et al. 2001; Gusnard and Raichle 2001). According to this hypothesis, the CEN would be able to suspend activity within the DMN, being related to intentional focus on specific features instead of the whole external environment (Buckner et al. 2008; Gusnard et al. 2001; Gusnard and Raichle 2001; Raichle et al. 2001). In addition, considering the detected interaction from the AN (RSN 5) not only to the DMN (RSN1) but also to the CEN (RSN 3), we suggest that the causal effect in this network may not be completely due to intrinsic activity during resting state, but could be possibly evoked by the noise from the scanner operation.

5 Conclusion

In summary, we focused on evaluating and understanding the possible effective connectivity within RSNs. We used ICA, a data-driven approach, to characterize RSNs from resting state fMRI data, and then CGCA to gain information about the causal influences among these RSNs. Our exploratory analysis confirmed the brain network architecture described in previous studies, and revealed that the self-referential network and the DMN have the highest positive and negative net causal flow, respectively. This suggests the two RSNs to be fundamental networks during the resting state, playing different roles in brain functional architectures. Such findings may enable new causality hypotheses to be generated for testing in future studies.

Acknowledgments This study was supported by grants from the Natural Science Foundation of China (90820006, 30770590, 30470510, and 30800264); the 863 Program (2008AA02Z408); and the key research project of science and technology of MOE (107097). DM was partly supported by the Flanders Research Foundation (FWO). YY was supported by the Intramural Research Program of the National Institute on Drug Abuse (NIDA), National Institute of Health (NIH), USA.

References

Achard S, Salvador R, Whitcher B, Suckling J, Bullmore E (2006) A resilient, low-frequency, small-world human brain functional network with highly connected association cortical hubs. J Neurosci 26:63–72

Amodio DM, Frith CD (2006) Meeting of minds: the medial frontal cortex and social cognition. Nat Rev Neurosci 7:268–277

Bartels A, Zeki S (2005) Brain dynamics during natural viewing conditions—a new guide for mapping connectivity in vivo. Neuroimage 24:339–349

Beckmann CF, DeLuca M, Devlin JT, Smith SM (2005) Investigations into resting-state connectivity using independent component analysis. Philos Trans R Soc Lond B 360:1001–1013

Biswal B, Yetkin FZ, Haughton VM, Hyde JS (1995) Functional connectivity in the motor cortex of resting human brain using echo-planar MRI. Magn Reson Med 34:537–541

Biswal BB, Van Kylen J, Hyde JS (1997) Simultaneous assessment of flow and BOLD signals in resting-state functional connectivity maps. NMR Biomed 10:165–170

Brovelli A, Ding M, Ledberg A, Chen Y, Nakamura R, Bressler SL (2004) Beta oscillations in a large-scale sensorimotor cortical network: directional influences revealed by Granger causality. Proc Natl Acad Sci USA 101:9849–9854

Buckner RL, Carroll DC (2007) Self-projection and the brain. Trends Cogn Sci 11:49–57

Buckner RL, Andrews-Hanna JR, Schacter DL (2008) The brain's default network: anatomy, function, and relevance to disease. Ann NY Acad Sci 1124:1–38

Calhoun VD, Adali T, Pearlson GD, Pekar JJ (2001) A method for making group inferences from functional MRI data using independent component analysis. Hum Brain Mapp 14:140–151

Chen Y, Bressler SL, Ding M (2006) Frequency decomposition of conditional Granger causality and application to multivariate neural field potential data. J Neurosci Methods 150:228–237

Chen S, Ross TJ, Zhan W, Myers CS, Chuang KS, Heishman SJ, Stein EA, Yang Y (2008) Group independent component analysis reveals consistent resting-state networks across multiple sessions. Brain Res 1239:141–151

Chen H, Yang Q, Liao W, Gong Q, Shen S (2009) Evaluation of the effective connectivity of supplementary motor areas during motor imagery using Granger causality mapping. Neuroimage 47:1844–1853

Corbetta M, Shulman GL (2002) Control of goal-directed and stimulus-driven attention in the brain. Nat Rev Neurosci 3:201–215

Cordes D, Haughton VM, Arfanakis K, Wendt GJ, Turski PA, Moritz CH, Quigley MA, Meyerand ME (2000) Mapping functionally related regions of brain with functional connectivity MR imaging. AJNR Am J Neuroradiol 21:1636–1644

Cordes D, Haughton VM, Arfanakis K, Carew JD, Turski PA, Moritz CH, Quigley MA, Meyerand ME (2001) Frequencies contributing to functional connectivity in the cerebral cortex in "resting-state" data. AJNR Am J Neuroradiol 22:1326–1333

Damoiseaux JS, Rombouts SA, Barkhof F, Scheltens P, Stam CJ, Smith SM, Beckmann CF (2006) Consistent resting-state networks across healthy subjects. Proc Natl Acad Sci USA 103:13848–13853

D'Argembeau A, Collette F, Vander Linden M, Laureys S, Del Fiore G, Degueldre C, Luxen A, Salmon E (2005) Self-referential reflective activity and its relationship with rest: a PET study. Neuroimage 25:616–624

De Luca M, Beckmann CF, De Stefano N, Matthews PM, Smith SM (2006) fMRI resting state networks define distinct modes of long-distance interactions in the human brain. Neuroimage 29:1359–1367

Dosenbach NU, Visscher KM, Palmer ED, Miezin FM, Wenger KK, Kang HC, Burgund ED, Grimes AL, Schlaggar BL, Petersen SE (2006) A core system for the implementation of task sets. Neuron 50:799–812

Dosenbach NU, Fair DA, Miezin FM, Cohen AL, Wenger KK, Dosenbach RA, Fox MD, Snyder AZ, Vincent JL, Raichle ME, Schlaggar BL, Petersen SE (2007) Distinct brain networks for adaptive and stable task control in humans. Proc Natl Acad Sci USA 104:11073–11078

Eckert MA, Kamdar NV, Chang CE, Beckmann CF, Greicius MD, Menon V (2008) A cross-modal system linking primary auditory and visual cortices: evidence from intrinsic fMRI connectivity analysis. Hum Brain Mapp 29:848–857

Fox MD, Snyder AZ, Vincent JL, Corbetta M, Van Essen DC, Raichle ME (2005) The human brain is intrinsically organized into dynamic, anticorrelated functional networks. Proc Natl Acad Sci USA 102:9673–9678

Fox MD, Snyder AZ, Zacks JM, Raichle ME (2006) Coherent spontaneous activity accounts for trial-to-trial variability in human evoked brain responses. Nat Neurosci 9:23–25

Fox MD, Zhang D, Snyder AZ, Raichle ME (2009) The global signal and observed anticorrelated resting state brain networks. J Neurophysiol 101:3270–3283

Fransson P (2005) Spontaneous low-frequency BOLD signal fluctuations: an fMRI investigation of the resting-state default mode of brain function hypothesis. Hum Brain Mapp 26:15–29

Friston KJ (1994) Functional and effective connectivity in neuroimaging: a synthesis. Hum Brain Mapp 2:56–78

Friston K (2009a) Dynamic causal modeling and Granger causality Comments on: the identification of interacting networks in the brain using fMRI: model selection, causality and deconvolution. Neuroimage

Friston KJ (2009b) Causal modelling and brain connectivity in functional magnetic resonance imaging. PLoS Biol 7:e33

Friston KJ, Frith CD, Frackowiak RSJ (1993) Time-dependent changes in effective connectivity measured with PET. Hum Brain Mapp 1:69–80

Friston KJ, Frith CD, Fletcher P, Liddle PF, Frackowiak RS (1996) Functional topography: multidimensional scaling and functional connectivity in the brain. Cereb Cortex 6:156–164

Gao Q, Chen H, Gong Q (2008) Evaluation of the effective connectivity of the dominant primary motor cortex during bimanual movement using Granger causality. Neurosci Lett 443:1–6

Geweke JF (1984) Measures of conditional linear dependence and feedback between time series. J Am Stat Assoc 79:709–715

Goebel R, Roebroeck A, Kim DS, Formisano E (2003) Investigating directed cortical interactions in time-resolved fMRI data using vector autoregressive modeling and Granger causality mapping. Magn Reson Imaging 21:1251–1261

Granger CWJ (1969) Investigating causal relations by econometric models and cross-spectral methods. Econometrica 37:424–438

Greicius MD, Krasnow B, Reiss AL, Menon V (2003) Functional connectivity in the resting brain: a network analysis of the default mode hypothesis. Proc Natl Acad Sci USA 100:253–258

Greicius MD, Srivastava G, Reiss AL, Menon V (2004) Default-mode network activity distinguishes Alzheimer's disease from healthy aging: evidence from functional MRI. Proc Natl Acad Sci USA 101:4637–4642

Gusnard DA, Raichle ME (2001) Searching for a baseline: functional imaging and the resting human brain. Nat Rev Neurosci 2:685–694

Gusnard DA, Akbudak E, Shulman GL, Raichle ME (2001) Medial prefrontal cortex and self-referential mental activity: relation to a default mode of brain function. Proc Natl Acad Sci USA 98:4259–4264

Hampson M, Peterson BS, Skudlarski P, Gatenby JC, Gore JC (2002) Detection of functional connectivity using temporal correlations in MR images. Hum Brain Mapp 15:247–262

Harrison L, Penny WD, Friston K (2003) Multivariate autoregressive modeling of fMRI time series. Neuroimage 19:1477–1491

Hyvarinen A (1999) Fast and robust fixed-point algorithms for independent component analysis. IEEE Trans Neural Netw 10:626–634

Jafri MJ, Pearlson GD, Stevens M, Calhoun VD (2008) A method for functional network connectivity among spatially independent resting-state components in schizophrenia. Neuroimage 39:1666–1681

Kelly AM, Uddin LQ, Biswal BB, Castellanos FX, Milham MP (2008) Competition between functional brain networks mediates behavioral variability. Neuroimage 39:527–537

Koechlin E, Summerfield C (2007) An information theoretical approach to prefrontal executive function. Trends Cogn Sci 11:229–235

Kwong KK, Belliveau JW, Chesler DA, Goldberg IE, Weisskoff RM, Poncelet BP, Kennedy DN, Hoppel BE, Cohen MS, Turner R et al (1992) Dynamic magnetic resonance imaging of human brain activity during primary sensory stimulation. Proc Natl Acad Sci USA 89:5675–5679

Li YO, Adali T, Calhoun VD (2007) Estimating the number of independent components for functional magnetic resonance imaging data. Hum Brain Mapp 28:1251–1266

Liao W, Marinazzo D, Pan Z, Gong Q, Chen H (2009) Kernel Granger causality mapping effective connectivity on fMRI data. IEEE Trans Med Imaging 28:1825–1835

Londei A, D'Ausilio A, Basso D, Sestieri C, Del Gratta C, Romani GL, Olivetti Belardinelli M (2007) Brain network for passive word listening as evaluated with ICA and Granger causality. Brain Res Bull 72:284–292

Lowe MJ, Mock BJ, Sorenson JA (1998) Functional connectivity in single and multislice echoplanar imaging using resting-state fluctuations. Neuroimage 7:119–132

Macrae CN, Moran JM, Heatherton TF, Banfield JF, Kelley WM (2004) Medial prefrontal activity predicts memory for self. Cereb Cortex 14:647–654

Mantini D, Perrucci MG, Del Gratta C, Romani GL, Corbetta M (2007) Electrophysiological signatures of resting state networks in the human brain. Proc Natl Acad Sci USA 104:13170–13175

Mantini D, Corbetta M, Perrucci MG, Romani GL, Del Gratta C (2009) Large-scale brain networks account for sustained and transient activity during target detection. Neuroimage 44:265–274

McKeown MJ, Jung TP, Makeig S, Brown G, Kindermann SS, Lee TW, Sejnowski TJ (1998) Spatially independent activity patterns in functional MRI data during the stroop color-naming task. Proc Natl Acad Sci USA 95:803–810

McKiernan KA, Kaufman JN, Kucera-Thompson J, Binder JR (2003) A parametric manipulation of factors affecting task-induced deactivation in functional neuroimaging. J Cogn Neurosci 15:394–408

Murphy K, Birn RM, Handwerker DA, Jones TB, Bandettini PA (2009) The impact of global signal regression on resting state correlations: are anti-correlated networks introduced?Neuroimage 44:893–905

Northoff G, Bermpohl F (2004) Cortical midline structures and the self. Trends Cogn Sci 8:102–107

Northoff G, Heinzel A, de Greck M, Bermpohl F, Dobrowolny H, Panksepp J (2006) Self-referential processing in our brain—a meta-analysis of imaging studies on the self. Neuroimage 31:440–457

Ongur D, Price JL (2000) The organization of networks within the orbital and medial prefrontal cortex of rats, monkeys and humans. Cereb Cortex 10:206–219

Raichle ME, MacLeod AM, Snyder AZ, Powers WJ, Gusnard DA, Shulman GL (2001) A default mode of brain function. Proc Natl Acad Sci USA 98:676–682

Roebroeck A, Formisano E, Goebel R (2005) Mapping directed influence over the brain using Granger causality and fMRI. Neuroimage 25:230–242

Roebroeck A, Formisano E, Goebel R (2009) The identification of interacting networks in the brain using fMRI: model selection, causality and deconvolution. Neuroimage

Salvador R, Suckling J, Coleman MR, Pickard JD, Menon D, Bullmore E (2005) Neurophysiological architecture of functional magnetic resonance images of human brain. Cereb Cortex 15:1332–1342

Seifritz E, Esposito F, Hennel F, Mustovic H, Neuhoff JG, Bilecen D, Tedeschi G, Scheffler K, Di Salle F (2002) Spatiotemporal pattern of neural processing in the human auditory cortex. Science 297:1706–1708

Seth AK (2005) Causal connectivity of evolved neural networks during behavior. Network 16:35–54

Sridharan D, Levitin DJ, Menon V (2008) A critical role for the right fronto-insular cortex in switching between central-executive and default-mode networks. Proc Natl Acad Sci USA 105:12569–12574

Stam CJ, Reijneveld JC (2007) Graph theoretical analysis of complex networks in the brain. Nonlinear Biomed Phys 1:3

Stark DE, Margulies DS, Shehzad ZE, Reiss P, Kelly AM, Uddin LQ, Gee DG, Roy AK, Banich MT, Castellanos FX, Milham MP (2008) Regional variation in interhemispheric coordination of intrinsic hemodynamic fluctuations. J Neurosci 28:13754–13764

Stevens MC, Kiehl KA, Pearlson G, Calhoun VD (2007) Functional neural circuits for mental timekeeping. Hum Brain Mapp 28:394–408

Stevens MC, Pearlson GD, Calhoun VD (2009) Changes in the interaction of resting-state neural networks from adolescence to adulthood. Hum Brain Mapp 30:2356–2366

Tian L, Jiang T, Liang M, Li X, He Y, Wang K, Cao B, Jiang T (2007) Stabilities of negative correlations between blood oxygen level-dependent signals associated with sensory and motor cortices. Hum Brain Mapp 28:681–690

Uddin LQ, Clare Kelly AM, Biswal BB, Xavier Castellanos F, Milham MP (2009) Functional connectivity of default mode network components: correlation, anticorrelation, and causality. Hum Brain Mapp 30:625–637

Upadhyay J, Silver A, Knaus TA, Lindgren KA, Ducros M, Kim DS, Tager-Flusberg H (2008) Effective and structural connectivity in the human auditory cortex. J Neurosci 28:3341–3349

van de Ven V, Formisano E, Prvulovic D, Roeder CH, Linden DE (2004) Functional connectivity as revealed by spatial independent component analysis of fMRI measurements during rest. Hum Brain Mapp 22:165–178

van de Ven V, Bledowski C, Prvulovic D, Goebel R, Formisano E, Di Salle F, Linden DE, Esposito F (2008) Visual target modulation of functional connectivity networks revealed by self-organizing group ICA. Hum Brain Mapp 29:1450–1461

van den Heuvel M, Mandl R, Hulshoff Pol H (2008) Normalized cut group clustering of resting-state FMRI data. PLoS ONE 3:e2001

Vincent JL, Snyder AZ, Fox MD, Shannon BJ, Andrews JR, Raichle ME, Buckner RL (2006) Coherent spontaneous activity identifies a hippocampal-parietal memory network. J Neurophysiol 96:3517–3531

Wilke M, Lidzba K, Krageloh-Mann I (2009) Combined functional and causal connectivity analyses of language networks in children: a feasibility study. Brain Lang 108:22–29

Wu CW, Gu H, Lu H, Stein EA, Chen JH, Yang Y (2008) Frequency specificity of functional connectivity in brain networks. Neuroimage 42:1047–1055

Zhou Z, Chen Y, Ding M, Wright P, Lu Z, Liu Y (2009) Analyzing brain networks with PCA and conditional Granger causality. Hum Brain Mapp 30:2197–2206